Video Article

Visualizing Clathrin-mediated Endocytosis of G Protein-coupled Receptors at Single-event Resolution via TIRF Microscopy

Amanda L. Soohoo[1], Shanna L. Bowersox[1], Manojkumar A. Puthenveedu[1]

[1]Department of Biological Sciences, Carnegie Mellon University

Correspondence to: Manojkumar A. Puthenveedu at map3@andrew.cmu.edu

URL: https://www.jove.com/video/51805
DOI: doi:10.3791/51805

Keywords: Cellular Biology, Issue 92, Endocytosis, TIRF, total internal reflection fluorescence microscopy, clathrin, arrestin, receptors, live-cell microscopy, clathrin-mediated endocytosis

Date Published: 10/20/2014

Citation: Soohoo, A.L., Bowersox, S.L., Puthenveedu, M.A. Visualizing Clathrin-mediated Endocytosis of G Protein-coupled Receptors at Single-event Resolution via TIRF Microscopy. *J. Vis. Exp.* (92), e51805, doi:10.3791/51805 (2014).

Abstract

Many important signaling receptors are internalized through the well-studied process of clathrin-mediated endocytosis (CME). Traditional cell biological assays, measuring global changes in endocytosis, have identified over 30 known components participating in CME, and biochemical studies have generated an interaction map of many of these components. It is becoming increasingly clear, however, that CME is a highly dynamic process whose regulation is complex and delicate. In this manuscript, we describe the use of Total Internal Reflection Fluorescence (TIRF) microscopy to directly visualize the dynamics of components of the clathrin-mediated endocytic machinery, in real time in living cells, at the level of individual events that mediate this process. This approach is essential to elucidate the subtle changes that can alter endocytosis without globally blocking it, as is seen with physiological regulation. We will focus on using this technique to analyze an area of emerging interest, the role of cargo composition in modulating the dynamics of distinct clathrin-coated pits (CCPs). This protocol is compatible with a variety of widely available fluorescence probes, and may be applied to visualizing the dynamics of many cargo molecules that are internalized from the cell surface.

Video Link

The video component of this article can be found at https://www.jove.com/video/51805/

Introduction

The process of clathrin-mediated endocytosis (CME) is dependent upon the well-timed arrival of the many components of the clathrin-mediated endocytic machinery to gather cargo and manipulate the plasma membrane into the vesicles[1-3]. CME is initiated by membrane deforming and cargo-adaptor proteins that come together at nascent sites of endocytosis[1]. These proteins recruit the coat protein clathrin, which assembles into a cage-like structure that forms the clathrin-coated pit (CCP)[4]. Once the CCP is fully assembled into a spherical shape, membrane scission, primarily through action of the large GTPase, dynamin, generates free clathrin-coated vesicles (CCVs)[5,6]. This internalization triggers rapid disassembly of the clathrin coat, allowing components to be re-used for multiple rounds of CME.

The discovery and characterization of the proteins involved in CME has been rooted in traditional biochemical, genetic, and microscopy techniques[4-6,8]. These assays have elucidated the roles and interaction points of these endocytic components. Although very useful for defining essential components of trafficking machinery, these assays are highly limited in capturing the dynamic behavior of CME components or cargo concentration. This is a critical limitation, since CME is driven by the choreographed assembly of sets of protein modules in defined steps, and since small changes in the dynamics of individual endocytic events can have large cumulative consequences on endocytosis. Further, recent data indicate that individual CCPs might differ both in composition and in behavior, suggesting that the physiological regulation of this process is highly spatially and temporally constrained[9-14]. Visualizing individual endocytic events, therefore, is essential to understand why there are multiple redundant proteins involved in CME and how these proteins might be controlled by physiological signals to regulate cargo internalization.

Here we describe the use of Total Internal Reflection Fluorescence Microscopy (TIRFM) to observe CME at the level of the dynamics of individual CCPs in living cells. TIRFM relies on the difference in refractive index between the glass coverslip and the fluid environment of cells[15,16]. When the excitation light is directed towards the cells at more than the critical angle, it is internally reflected, creating an evanescent wave that maintains a thin field of illumination extending approximately 100 nm above the coverslip. This ensures that only the fluorescent molecules within this narrow field are excited. Practically, this allows the excitation of fluorescent molecules on or near the plasma membrane, and minimizes fluorescence from the interior parts of the cell. This provides a significantly higher signal-to-noise ratio and z-axis resolution to visualize events at the plasma membrane, compared to more commonly used modes such as conventional epifluorescence or confocal fluorescence microscopy. We also describe, at an introductory and practical level, the use of a commonly used image analysis platform to analyze and quantitate simple morphological features and dynamics of individual cargo endocytic events.

Protocol

1. Expression of Fluorescently Tagged CME Components in Cultured Cells

HEK293 cells are useful model cells that have been used extensively to study GPCR biology and endocytosis, and therefore are used as models in this protocol. Use any transfection protocol providing uniform expression without overexpression and low cytotoxicity.

1. Handle all cell culture in a sterile laminar flow hood. Fill 4 wells of a 12-well plate with 1 ml of Dulbecco's Modified Essential Media (DMEM) with 10% Fetal Bovine Serum (FBS). From a confluent T25 flask of HEK293 cells dilute 1:50, 1:25, 1:16, 1:10 respectively into each of the 4 wells.
    1. Alternatively, seed cells to a multi-well plate of desired size, as per manufacturer's instructions. Seed 0.4 - 2 x 10^4 cells into a 12-well plate. Grow the cells overnight in a sterile 37 °C with 5% CO_2 and 95% humidity.
    NOTE: Considering that growth rates vary depending on the conditions and cell lines, it might be preferable to seed multiple wells to ensure ideal confluency for transfection the next day or the possibility of performing transfections in duplicate.
2. The next morning, select a well that is ~70% confluent for transfection (see **Figure 1B**). If no well has reached this state, wait another day.
NOTE: 70% confluency is ideal for HEK293 cells. Transfecting cells that are more sparse results in cell death and toxicity. Transfecting over-confluent cells results in poor expression.
3. Add 60 µl buffer EC (from transfection kit), 400 ng of plasmids encoding tagged GPCRs and/or components of the clathrin machinery, and 2.4 µl of Enhancer into the 1.5 ml microcentrifuge tube, as described in the manufacturer's protocol. Vortex for 2 sec to ensure sufficient mixing, and spin in a microfuge at 2,000 x g for 2 sec to collect the liquid at the bottom.
4. Add 6 µl Effectene as described in the manufacturer's protocol. Vortex for 2 sec, and spin at 2,000 x g for 2 sec in a microfuge to collect the liquid at the bottom. Wait for 20 min to allow for formation of transfection complex micelles.
5. Aspirate media from the well to be transfected. Gently add 0.8 ml of DMEM with 10% FBS to the transfection reagent mixture and mix by pipetting up and down slowly to reduce breaking the micelles. Add the media and transfection mixture to the well very slowly from the side. Add any remaining transfection mixture from the microcentrifuge tube to the well using a micropipettor.
NOTE: Optionally, add an extra 0.5 ml of DMEM with 10% FBS to the transfected well to give the cells extra nourishment resulting in gentler transfection and lower transient expression.
6. Return the cells to the 37 °C incubator for 5 hr.
7. Aspirate media containing the transfection mixture. Replace with 1 ml of DMEM with 10% FBS. Allow the cells to grow overnight.
8. The next day, pass the cells to uncoated coverslips, previously sterilized by autoclaving.
    1. Add 0.5 ml of Phosphate Buffered Saline (PBS) with 1 mM EDTA to each well. Alternatively, use 0.5 ml of 0.05% Trypsin-EDTA. Leave in the incubator for 1 min.
    2. Place 3 round, sterile 25 mm coverslips into separate wells of a 6-well plate. Fill each well with 2 ml of media. Gently push the coverslip down to the bottom of the well to prevent cells from growing on the bottom of the coverslip.
    3. Manually agitate the well to lift off the cells from the bottom of the well. Add 1 ml of DMEM with 10% FBS to resuspend. Distribute the lifted cells from 1 well of a 12-well plate evenly among the 3 coverslips. Alternatively, plate cells on 3 glass-bottomed dishes.
9. Allow the cells to grow on the coverslips for at least 48 hr before imaging. Ensure that cells are spread out and flat.

2. Imaging CCP and Cargo Dynamics Using TIRFM

1. Conjugate M1 anti-FLAG antibodies with Alexa dyes using Alexa Fluor Protein Labeling kit according to the manufacture's protocol. Alternatively, pre-conjugated antibodies may be purchased.
2. Pre-incubate cells with the antibodies at a 1:1,000 dilution in 1 ml of pre-warmed Leibovitz medium with 10% FBS, or Opti-MEM with 50 mM HEPES pH 7.4 and 10% FBS for 10 min at 37 °C (imaging medium), to label FLAG-tagged GPCRs on the cell surface. Skip these steps if genetically encoded fluorescent proteins, such as GFP, are used as tags (see discussion for details).
3. Transfer the coverslip to a live-cell imaging chamber. Alternatively, for glass-bottomed dishes, aspirate antibody-labeling media and add 700 µl of pre-warmed imaging medium.
    1. Use a pair of forceps and bend the tip of a 25 gauge needle into a hook.
    2. Hold a pair of forceps in the dominant hand. Hold the bent needle in the other. Turn the needle until the hook curves down towards the glass. Gently drag the needle, hook side down, across the bottom of a 6-well plate until it hooks onto the coverslip. Take care to not scratch the surface of the coverslip, as it will detach cells. Gently lift the coverslip up from the bottom of the well. Balance the coverslip against wall of the well for support.
    3. Use the forceps to grasp near the edge of the coverslip and move the coverslip cell side up to the imaging chamber, and assemble the chamber. Add 700 µl (or appropriate amount) of pre-warmed imaging medium. Handle the coverslips carefully without pressure to prevent cracking or breaking.
4. Transfer the chamber onto the microscope and keep the temperature of the cells at 37 °C using a stage heater or an enclosed incubator.
5. Bring cells into focus using a 100X or 60X TIRF oil-immersion objective (1.45 NA or above). Image the cells in conventional epifluorescence or confocal modes of illumination (*i.e.* not TIRFM) to identify cells expressing the appropriate constructs. Out-of-focus cells are nearly invisible in the thin depth of TIRF illumination making it difficult to find the focal plane and cells.
NOTE: Some systems use the same lasers for TIRFM to image in conventional epifluorescence, by moving the angle of incidence of the laser above the critical angle. As an important safety precaution, always be aware of the angle of the laser beam, and always direct it away from the observer.
6. Focus down to the bottom surface of an expressing cell until the outline of plasma membrane around the cell disappears and the center of the cell appears. This is most apparent with a plasma membrane localized cargo protein such as the µ-opioid receptor (see **Figure 2A**).

7. Switch to TIRF imaging.
    1. If using the same lasers for imaging in conventional epifluorescence, increase the angle of incidence of the laser until out-of-focus fluorescence in the interior of the cell disappears, and no outline of plasma membrane around the cell is seen. (Compare **Figure 2C** to **Figures 2A** and **2B**)
    NOTE: In TIRFM, moving the focal plane causes the image to go completely out of focus and/or dim, and the overall fluorescence levels decreases due to the smaller depth of illumination. Therefore, an alternate method to switch to TIRFM illumination is to first focus on the center of the cell in confocal/conventional epifluorescence, then increase the angle of incidence until you lose most of the fluorescence, and then focus down to the plasma membrane.
    2. Once in TIRFM, ensure the excitation laser reflects back through the objective and is not visible above the objective. Confirm this by checking if the laser spot is visible.
    NOTE: In conventional epifluorescence or confocal modes, the laser illumination is visible above the objective, such as on the ceiling.
    3. Refine the focus to get a crisp image. The main components of the endocytic machinery, such as clathrin, will be visible in puncta. Adjust the focus on fine, so the puncta are as round as possible.
    NOTE: For membrane-localized cargo, adjust the fine focus until the filopodia appear distinct.
    4. Use an acquisition program to save all the imaging parameters such as mirrors and TIRF angle. Do this for all necessary wavelengths.
8. Scan around the coverslip to find cells expressing all desired endocytic markers: the μ-opioid receptor and the adapter β-arrestin in the example shown in **Figure 3A**. Select cells that are expressing but not over-expressing. See discussion for details.
9. Once cells are identified, acquire images every 3 sec for 10 min. This is sufficient to capture the lifetime of a CCP, since the average lifetime of a CCP in HEK293 cells imaged under these conditions is around 40 sec[10-11]. This allows about 12-14 frames to observe the CCP. For example see **Movie 1**. Repeat all steps to image additional cells.

3. Analysis of Endocytic Dynamics by Manual Verification

Although manual verification of CCP lifetimes is greatly limited by the number of CCPs that can be detected, it still remains an accurate means of detection undeterred by global changes in the image and detection artifacts. See discussion for details.

1. Open the file in ImageJ. Images are stored as a single stack of tiff files with interleaved channels. Convert images to hyperstacks. Go to Image > Hyperstacks > Stack to Hyperstack. Enter the number of channels acquired (*i.e.* if imaging β-arrestin and the μ-opioid receptor, enter 2), Enter 1 for Z stack (TIRFM is a single plane), and the number of frames of the movie (*i.e.* a 10 min movie at 1 frame every 3 sec is 200) in the pop-up window.
2. The hyperstack format yields a window with two scroll bars. Use the top bar to move through the channels and the bottom to move through time. Scroll to the channel of the protein whose lifetimes will be assayed.
3. Move to frame 10 or 15 of the movie to reduce the inclusion of pre-existing CCPs whose entire durations are not visible. Draw an ROI box around a spot chosen at random.
4. Count the number of frames a spot is visible.
NOTE: See **Figure 3B** and **3C** for examples of three morphological categories of endocytic events[10,11,16-19].

4. Analysis of Endocytic Dynamics by Objective Recognition

Objective recognition allows detection of virtually all of the imaged CCPs in a cell, but can be prone to error due to spurious detection of erroneous structures. See discussion for details weighing the advantages and disadvantages of each method. Several programs, including custom-built algorithms, may be used to objectively detect CCPs. This protocol describes objective recognition of CCPs using Imaris, an image-analysis software (see **Materials**).

1. To begin, open the raw image file in the image-analysis software. By default, a merged color image appears. Use the “Display Adjustment” window to adjust the brightness of a channel. Click on the name of a channel to change the displayed color. Uncheck the box next to the channel to prevent its display (See **Figure 4A**).
2. Create “Spots” by clicking on the icon with orange spots. See **Figure 4B**. Select a Region of Interest (ROI) around the cell. See **Figure 4C**. Use a ROI to exclude areas that will incorrectly detect bright leading edges and plaques. Analyze multiple cells with different expression levels separately.
3. Measure the diameter of a Spot to provide initial estimates for the algorithm. Switch to “Slice” mode, and click on polar ends of a spot to measure its diameter. See **Figure 4E**. Do this for 4 or 5 round Spots that look indicative of a CCP at the height of its stability, after formation and before scission. Use these measurements to calculate average diameter down to the nearest tenth of a micron.
4. Detect Spots. Return to “Surpass” mode. Select the appropriate channel for detection. Enter the average measured diameter, usually 0.3 or 0.4 μm. Click the blue forward arrow to quantify the Spots. See **Figure 4E**. If the diameter of Spots is underestimated, spurious points of fluorescence will be identified as Spots. If the diameter is too large, true Spots will be ignored. When unsure, estimate a little bit lower, and filter out the incorrect detections later.
5. Filter Spots by Quality. Adjust the filter to capture as many Spots as possible without background. The Quality filter is selected by default[20]. See **Figure 4F**.
    1. Use the “Quality” curve as a guide to set an appropriate threshold. Move the bottom threshold of the filter with the left mouse button to this first dip in the curve. This is a good starting point for the filter, as this position usually refines detection to only visible Spots. See **Figure 4F**.
    2. Detected Spots appear on the movie as spheres or center pixels. Using the “Colors” tab, adjust the color of the Spots to a contrasting color to make it easier to see them. Scroll through the movie to review the Spots in each frame. The goal is to detect as many Spots as possible for the entirety of their lifetimes.
    3. Eliminate dimmer Spots or manually connect them into continuous tracks later on, as they are not detected well through the course of their lifetimes.

4. Remove bright plaques with an “Intensity” filter, if required. Click the green plus sign to add a new filter. See **Figure 4F**. Create an Intensity filter to filter in or out Spots of a given fluorescence signals. Use the generated Intensity curve, (analogous to Quality Curve discussed in 4.5) to set the threshold. Use the left mouse button to remove the extreme left end of the curve that represents the brightest Spots.
   NOTE: Large plaque structures are usually among the brightest elements in the cell, and they are easily excluded with this filter.
5. Scroll through the movie to ensure that the CCPs are detected as Spots and the brightest plaques are no longer detected. **Figure 3D** shows a cell where detection of CCPs (denoted by white spheres) was optimized with the quality filter and plaques were excluded with the quality filter.
6. Reduce bright cell edges with the quality filter. Bright objects may still need to be removed manually, at the next step. Continue with the blue arrow.
7. Remove aberrant Spots in the Edit Spots screen. Switch to “Select” mode. Click on the spot. It will turn yellow. Click “Delete”. Click the blue arrow to continue building the algorithm. See **Figure 4G**.

6. Measure tracks. Set tracks to “Brownian motion.” The CCP should not exhibit any directed movement, only minimal drifting across the plasma membrane. This algorithm is most appropriate for that motion. See **Figure 4H**.
   1. Set the Max Distance to a small value such as 0.7 µm. See **Figure 4H**.
      NOTE: Setting a small distance minimizes connection of adjacent Spots and still allows for continued tracking of a cell spot through CCP or cell movement.
   2. Set Max Gap Size to 1. This allows a track to continue if there is only one frame missing in succession. Click the blue arrow to calculate tracks. See **Figure 4H**.
      NOTE: Gap sizes of more than 3 causes different tracks to be incorrectly linked together.
   3. Switch track viewing to “Dragon Tail.” Scroll through the movie observing the detection quality. If adjacent Spots are being connected, decrease the Max Distance below 0.7 µm. If Spots are being broken up too readily, increase the Max Gap Size. Click the blue arrow to create tracks. This leads to the filter tracks screen. See **Figure 4H**.

7. Filter Tracks and Export Data. Use an “Intensity” filter to remove additional bright plaques. Use a “Displacement” filter to remove endosomes that enter the TIRF field. Use caution, as longer Spots will have longer displacements as well. Click the green double arrow to complete the protocol. See **Figure 4I**.
   1. Use the Edit Tracks tab, with the pencil icon, to remove false positive detections of Tracks that could not be removed by filters. Check for discontinuities or false connections. To connect two tracks, select them using Ctrl-Left-Click, then click on “Connect” in the Edit Tracks box. To disconnect tracks into separate spots, select a track and hit “Disconnect”. Select multiple Spots with Ctrl+Left-Click and click “Connect” to create a new Track. The method is the same for Editing Spots, described in **4.5.7**. See **Figure 4J**.
   2. To export data, go to the statistics tab. Click on the single floppy disk icon to export the selected statistic. Click on the icon that looks like a series of floppy disks to export all statistics. The “Track Duration” statistic contains the length of the endocytic tracks. See **Figure 4K**.

Representative Results

Using live-cell TIRF Microscopy we have recorded the endocytic dynamics of the µ-opioid-receptor (MOR), a G-protein coupled receptor (GPCR) and its endocytic adaptor protein β-arrestin. The β-arrestin construct was transiently transfected into a stably expressing MOR cell line using the protocol outlined in **Figure 1**, and imaged 96 hr later. The MOR in the stable cell line is N-terminally tagged with a pH-sensitive GFP. This fluorescent protein only fluoresces in the neutral extracellular fluid. Also, the MOR only endocytoses once activated by an agonist, and remains otherwise evenly distributed across the plasma membrane. Focusing on the adherent plasma membrane that is sitting on the cover-glass in confocal mode results in a cell that is filled in with a dim fluorescence. This is different from a focusing on the center of the cell, where the plasma membrane is only seen as a ring of fluorescence around the cell. Compare the left and right panels in **Figure 2A**. Switching to conventional epifluorescence or TIRF with an incorrect angle causes out of focus fluorescence to become apparent in the same cells as shown in **Figure 2B**. When the TIRF angle is correct the plasma membrane is very crisp, clear and bright and out of focus fluorescence no longer disrupts the image. Compare **Figure 2C** to **Figures 2A** and **2B**.

The image is clear and sharp because the MOR is on the adherent plasma membrane, which is largely within the TIRF field. In contrast, β-arrestin remains in a cytosolic pool when not yet recruited to endocytic puncta, and appears hazy and out of focus because it is not in the TIRF field. Once the MOR is activated by an agonist, β-arrestin is recruited to the plasma membrane, and both β-arrestin and the receptor redistribute to CCPs (**Figure 3A** and **Movie 1**, β-arrestin in green, MOR in red, overlay is yellow).

The lifetimes of these clusters can be quantified manually using the three parameters for completed endocytosis as depicted in **Figure 3B**. The spots denoting CCPs can either disappear completely (also see **Figure 3C**), “blink” on and off or “pinch off” a larger structure. The latter two conditions represent events that are spatially too close together to be resolved as separate events. The Spot detection algorithm in Imaris is also useful to quantify CCPs, as outlined in **Figure 4**. **Figure 3D** denotes CCPs detected using Imaris, after filtering to remove non-dynamic plaque structures. Overlaid white spheres denote detected spots. Dimmer spots that could not be detected for their whole lifetimes were also excluded with the “Quality” filter.

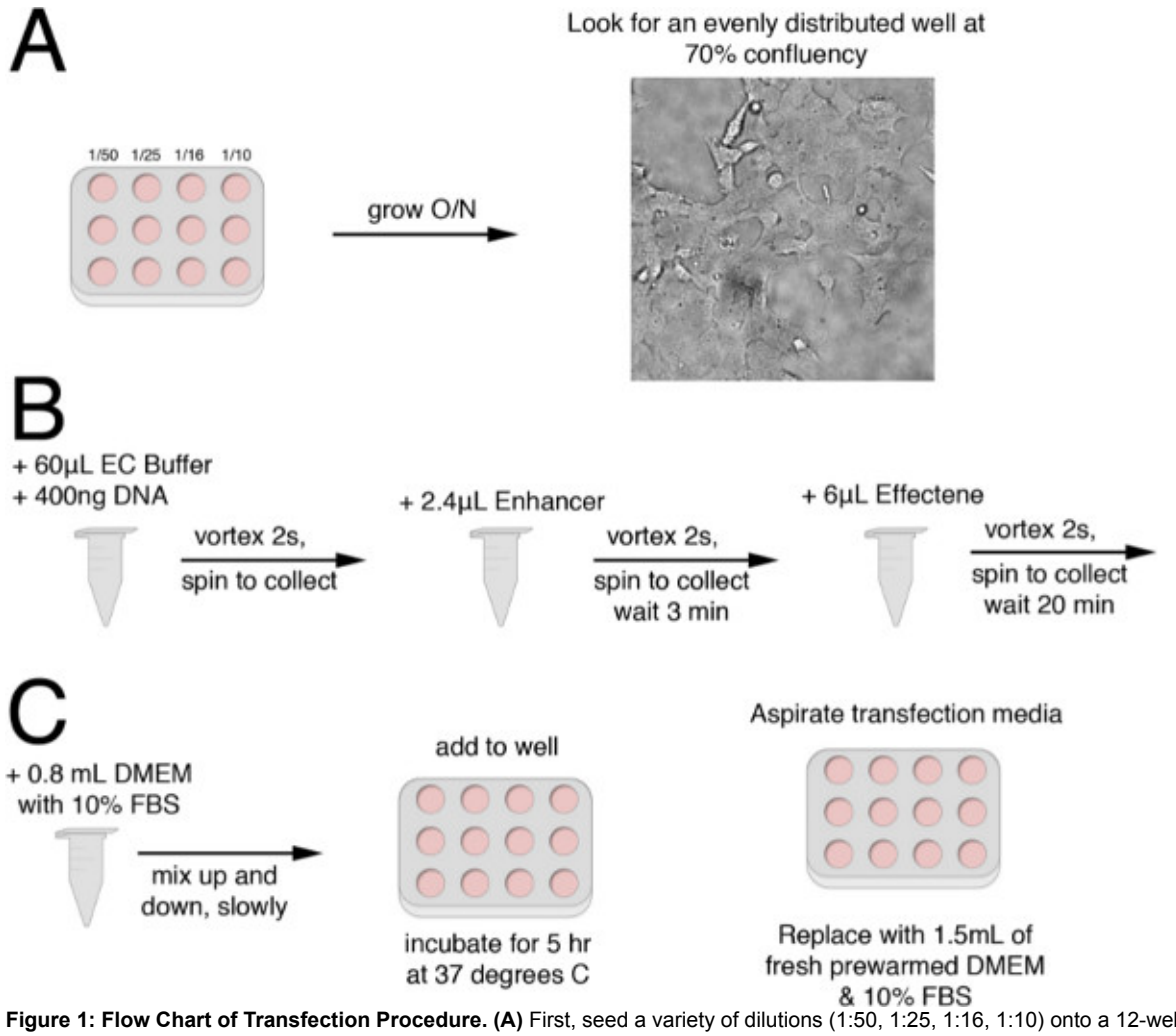

Figure 1: Flow Chart of Transfection Procedure. (A) First, seed a variety of dilutions (1:50, 1:25, 1:16, 1:10) onto a 12-well plate. Allow cells to grow overnight. The next day, look for a well that is about 70% confluent, and evenly distributed, as depicted. This is the well that will be transfected. **(B)** Add 60 µl of EC buffer and 400 ng of DNA into a microcentrifuge tube. Vortex for 10 sec and spin the liquid to bottom of the tube. Add 2.4 µl of Enhancer. Vortex for 2 sec and spin the liquid to bottom of the tube. Incubate at room temperature for 3 min. Add 6 µl of Effectene. Vortex for 2 sec and spin the liquid to bottom of the tube. Incubate at room temperature for 20 min. **(C)** Slowly mix 0.8 ml of DMEM with 10% FBS with the transfection. Add to cells in previously selected well. Incubate cells for 5 hr at 37 °C. Replace with fresh DMEM with 10% FBS.

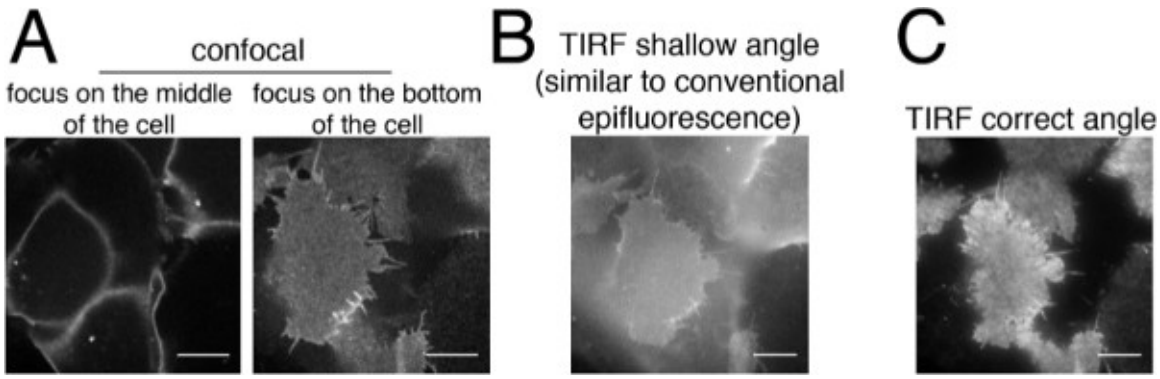

Figure 2: Finding the TIRFM field. (A) The plasma membrane imaged in confocal. The left panel depicts cells in confocal with a focus on the center of the cell. The plasma membrane is only seen as a "ring" around the cell. Focusing down to the basal plasma membrane, adjacent to the coverslip causes the cell to be filled in with a dim fluorescence. The plasma membrane "ring" should not be visible in the thinner TIRF field. **(B)** The basal plasma membrane with a shallower TIRF angle producing conventional epifluorescence illumination through the sample. This illuminates the entire cell and much out of focus fluorescence from the top of the cell is present. **(C)** The plasma membrane in TIRF. Focusing on filopodia helps to find this plane. Notice that it is a smooth single plane. Scale bars are 10 µm. Please click here to view a larger version of this figure.

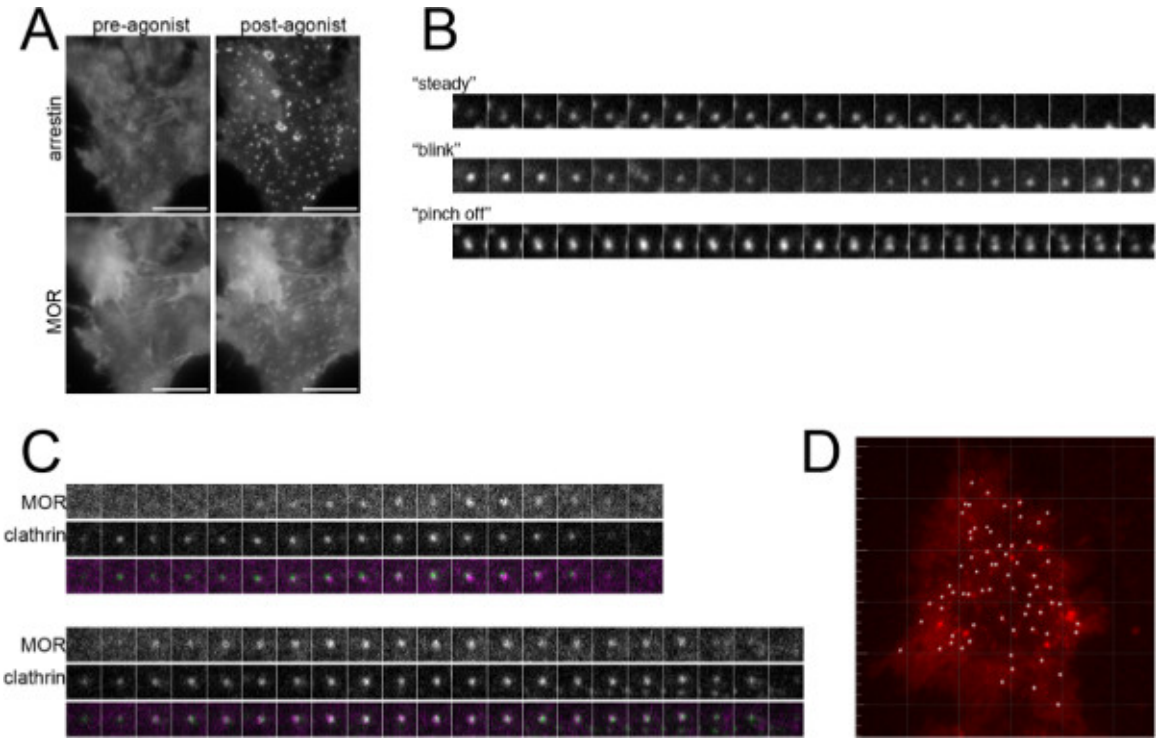

Figure 3: Visualizing and Quantifying Endocytic events in TIRF. (A) A cell expressing the μ-opioid-receptor (MOR) and β-arrestin before and after addition of an agonist that induces endocytosis. The agonist causes redistribution of both proteins to endocytic puncta. Scale bar is 10 μm. **(B)** Three types of endocytic events, seen by visualizing arrestin dynamics, consistent with previously described morphologies. "Steady", one steady signal that rapidly disappears. This is the main type, indicating that the CCP has budded and left the TIRF field. "Blink", a signal that blinks to a lower signal and reappears at the same spot due to assembly of a second CCP at the same spot. "Pinch off", a tubular projection comes off a spot, when two CCPs are too close to each other to be resolved as distinct spots, and one is endocytosed. The box is 2 x 2 μm. **(C)** Visualizing clathrin-mediated endocytosis of MOR at single-event resolution. Two examples that represent the major fraction of MOR endocytic events are shown. Frames are every 3 sec. The box is 2 x 2 μm. **(D)** Detection of individual endocytic events using Imaris. White spheres denote CCPs detected as Spots. Spot detection was optimized using a "Quality" filter. Dimmer spots that could not be detected for the entirety of their lifetimes were also excluded with the quality filter. Large plaque structures that are shown as being undetected were omitted using an "Intensity" filter. Please click here to view a larger version of this figure.

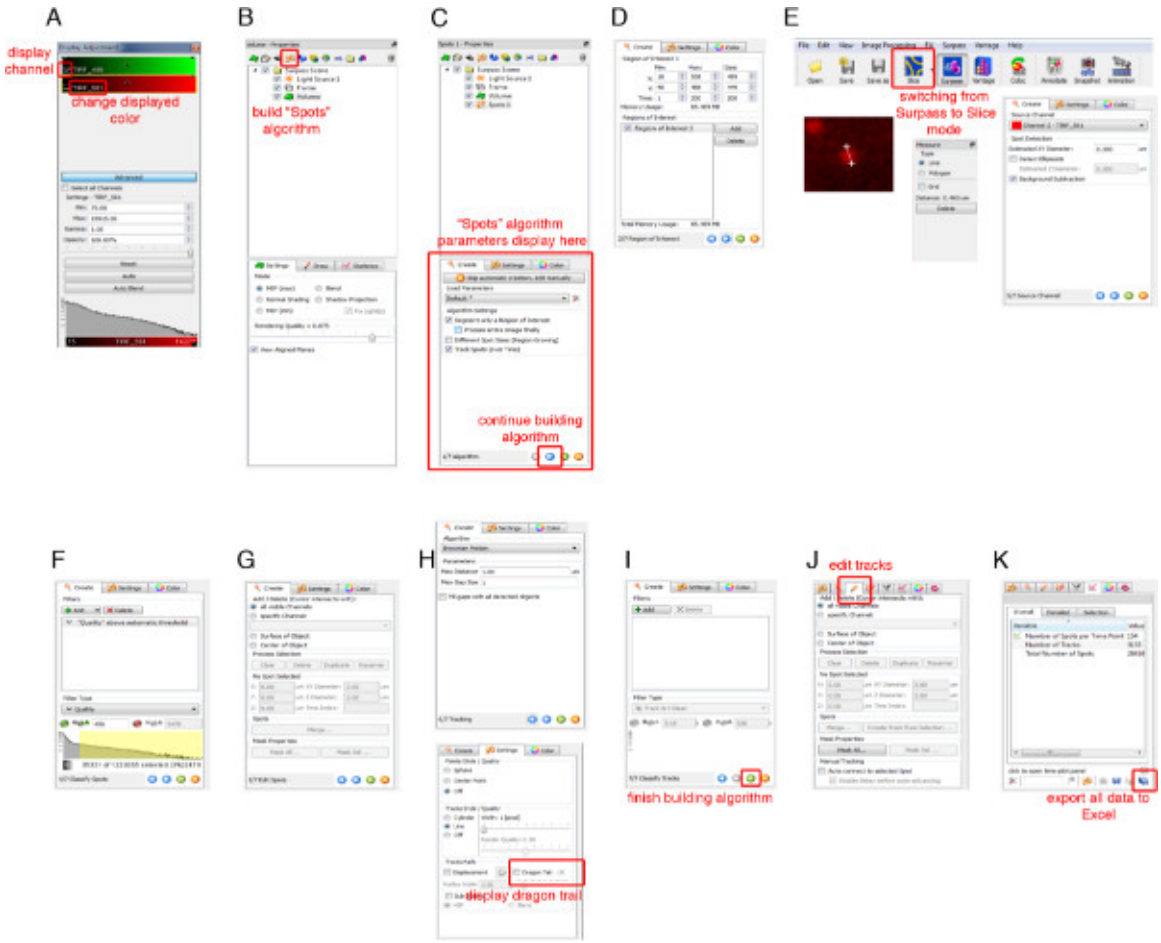

Figure 4: Objective Recognition of the Dynamics of Endocytic Events using Imaris. (A) The Display Adjustment window, used to adjust the display of the image as described in **Step 4.1**. **(B)** Opening the "Spots" algorithm builder. The builder is displayed in the window below. **(C)** The first step of the Spots algorithm builder. Check "Track Spots (over Time)." Check "Segment only a Region of Interest," if needed. **(D)** ROI selection screen. See **Step 4.2** for details. **(E)** The multiple windows needed to define the diameter of a measured Spot. Panels represent: switching from Surpass to Slice mode using the Navigation Bar at the top, clicking on the polar ends of a spot, where the measured diameter displayed, typically on the far right hand side, where to enter the measured diameter. See **Steps 4.3-4.4**. **(F)** The spot Quality Filter described in **4.5-4.5.3**. **(G)** Edit spots window described in **4.5.7**. **(H)** Measure tracks and viewing tracks windows, described in **4.6**. **(I)** Filter Tracks window described in **4.7**. **(J)** Edit tracks window described in **4.7.1**. **(K)** Save data screen described in **4.7.2**. Please click here to view a larger version of this figure.

Movie 1. Example movie of live cell TIRF Microscopy of MOR clustering and endocytosis. β-arrestin is shown in green, the MOR is shown in orange. Neither protein is localized to CCPs before agonist stimulation of the MOR. Once the MOR is activated, both β-arrestin and MOR cluster in CCPs, seen as distinct puncta that can be analyzed individually for their properties.

Discussion

Here we describe the use of TIRFM to visualize clathrin-mediated endocytosis (CME) at the level of individual CCPs in living cells in real time. CME is a rapid and highly dynamic event mediated by the cumulative effect of many spatially and temporally separate individual events. Most assays that are currently used, such as biochemical measurements of internalization using surface biotinylation or ligand binding, flow-cytometry or fixed cells assays measuring amount of internalized proteins, or electron microscopic localization of proteins, monitor ensemble changes in protein localization at fixed time points. These existing methods have been very useful in identifying proteins that are necessary for CME, but lack the spatial and temporal resolution that matches the physiological scales of CME or other dynamic membrane trafficking processes. This is important, as recent evidence suggests that CCPs are heterogenous in their protein composition and dynamics[9-12], and as CME is likely rapidly regulated in a spatially discrete manner. Live cell TIRFM provides the ability to analyze CME at the level of spatially separated single CCPs, in real time, in living cells.

Successful application of this powerful assay relies on two key factors: good health of the cells and thorough analysis of the parameters of CME. For the former, proper expression of tagged proteins and microscopy techniques minimizing phototoxicity are critical. Cell lines stably-expressing the proteins of interest are ideal, as the expression levels can be reliably estimated. We tag the receptors with either N-terminal Flag epitope or SpH tags[21-25]. While not strictly necessary, both labeling systems facilitate TIRFM of CME because receptors can be selectively detected on the plasma membrane at the start of the experiment. The desired additional endocytic components may also be transiently transfected into these stable cell lines. The transfection protocol noted here is optimized for imaging CME using TIRFM. First, it is tailored for even and moderate levels

of expression. Poor expression necessitates higher laser power for detection and increases the risk for both phototoxicity and photobleaching. Further, since this assay records the disappearance of puncta as internalized CCPs, low signals and photobleaching are detrimental also to analysis. We suggest that, under these circumstances, the total duration and/or the frequency of imaging be reduced. Second, the short incubation of the transfection reagents on the cells, the interval between transfection and the experiment, and the fresh passage of transfected cells to coverslips before imaging, all ensure that the imaged cells are in optimal health. Third, this ensures that the majority of clathrin structures are CCPs, and not flat sheets of clathrin or clathrin plaques. Fourth, this protocol minimizes over-expression of transfected CME components, which has been shown to alter CME dynamics[20,26].

For imaging with low phototoxicity, it is important to optimize the imaging system for optimal resolution and maximum sensitivity. The magnification of the objective and the camera detector size should be matched to minimize under- or oversampling and empty magnification. A high numerical aperture (1.45 or above) TIRF objective should be used to collect the maximum light possible. We acquire images with an electron-multiplying charge coupled device camera for high quantum efficiency, low exposure times, and fast readout speeds. Additionally, to ensure the health of the cells, they are imaged in Leibovitz media, which is buffered independent of CO_2, and is supplemented with 10% FBS, in a fully enclosed chamber set to 37 °C. Because TIRFM is highly sensitive and the high numerical aperture objectives used can detect even minimal ambient light, it is critical to create an enclosed imaging environment free from external light and vibrations that may disrupt the fine focal plane.

It is important to note that the absolute lifetimes and dynamics of most components of CME vary heavily depending on cell types, expression levels of proteins, temperature, days after plating, and other variations in culture conditions[7,10,14,17,20,25,27]. This is reflected in the huge variations in the timescales and distributions observed between different groups using this technique, a clear limitation of this assay. Further, it is possible that CCPs on the bottom surface of the cell, imaged in TIRFM, behave differently from the top surface[23,25]. While it is debatable as to which surface accurately represents a 'typical' cell surrounded by extracellular matrix components in a tissue, interpretations of CCP dynamics seen by this technique need to consider this potential difference. The true strength of the assay, therefore, lies in comparing changes in dynamics of CCPs, in the same cells under identical culture conditions, after acute manipulations, including the clustering of cargo molecules such as GPCRs in response to activation. This comparison allows for normalization of the changes to the same cell, thereby controlling for all the parameters mentioned above that might induce variations in CCP behavior.

We typically employ both manual and automated analyses, described above, to analyze the duration of endocytic events: manual verification and objective recognition using the Imaris image analysis software. Manual verification is labor- and time-intensive, as it is limited by the number of CCPs a user can count, but it is arguably the most accurate technique available. A trained human eye can easily continue to track a CCP through cell movement, and changes in shape or focus, accurately excluding plaques and defective pixels. It can also detect morphological changes in the CCP indicative of completed events, as shown is **Figure 3B** and **3C**. It is imperative, however, that the analysis remains objective as possible within these constraints. This requires the definition of specific criteria that are used consistently across all data sets. In addition, we typically analyze images in a double-blind manner, where the image names are scrambled so that the conditions remain unknown to the person analyzing the images. Automated detection, *e.g.* using the “Spots” and “Track Duration” algorithms in Imaris, can be used to detect most of the endocytic spots in a given movie, generating a high sample number. While many options, including highly complex custom-made algorithms[3,14,23,26,27], are being generated, the reliability of these methods to detect correct endocytic events while avoiding spurious detection remains the biggest concern. For example, in Imaris, cell movement creating bright leading edges, plaques, and out of focus frames can easily throw off the spot-detection algorithm, as it has a tendency to detect bright structures as being composed completely of spots. In order to prevent these Spots from being connected into a track, they must all be removed. Single aberrant Spots that are not in large structures such as plaques may be removed with the Edit Spots tab, while Spots connected may be removed later using the Edit Tracks tab. The aberrant spots can also be removed with custom filters. For example, **Figure 3D** shows an intensity filter used to limit avoid including plaques in CCP detection. The Quality filter is another very useful filter for deleting erroneous spots. “Quality” is a cumulative measurement of brightness and shape found by taking the fluorescence intensity of the spot and Gaussian filtering by ¾ of the length of the spot radius[20]. The Quality curve is found underneath the selected filters. It depicts the number of spots (y) detected when the quality is a certain value (x). The lower the quality, the more spots detected. If the quality filter is too low, spots will be detected where there is no visible fluorescence, conversely, if the quality filter is too high, only the brightest spots will be detected. Follow along the curve towards greater values (x); the number of spots detected (y) will typically drop dramatically. Move the bottom threshold to this point. This is the minimum point to place the bottom threshold. Other major contributors to false spots in the TIRF field are endosomes that move to the periphery of the cell and enter the TIRF field. A robust criterion for removing these is the mobility of spots, *i.e.* the displacement of spots over time. CCPs move very little unless as part of the movement of the whole cell, while endosomes exhibit fast Brownian or directed movement. Newer algorithms, while significantly improved, are still being refined and optimized[3,14,23,26,27]. As these methods become more sophisticated and reliable, we can analyze hundreds or thousands of spots, without having to manually verify them at each point. Currently, however, we suggest that these two analyses be used together to complement each other for accuracy.

The protocol we have described can be easily adapted to answer many questions regarding cargo endocytosis. It can be used to perform simple co-localization of cargos with CME components, and used to show changes on specific components of the endocytic machinery due to particular stimuli. The assay can also easily be adapted for any endocytic process, such as caveolae[28], that show discrete concentrations of cargo and coat components, and to the study of these fundamental processes in specialized cell types. In the future, as genome editing becomes more mainstream[20,29,30], we anticipate that it will become the preferred method for tagging components, and that the dynamics and behavior of various components will be refined further. Considering that our understanding of cellular processes has been largely driven by the identification of genes, protein modifications, and interactomes, the assay we described here represents one of the next frontiers of enquiry, viz. the definition of the spatiotemporal dynamics of these processes and mechanisms.

Disclosures

The authors have nothing to disclose.

Acknowledgements

The authors would like to thank Drs. C. Szalinski, H. Teng, and M. Bruchez for help with Imaris, R. Vistein, and D. Shiwarski for technical help and advice, and Dr. M von Zastrow, Dr. T Kirchhausen, Dr. D Drubin, and Dr. W Almers for reagents and helpful discussion. Funding provided by T32 grant NS007433 to SLB and NIH DA024698 and DA036086 to MAP.

References

1. McMahon, H. T., & Boucrot, E. Molecular mechanism and physiological functions of clathrin-mediated endocytosis. *Nature Reviews Molecular Cell Biology.* **12** (8), 517–533, doi:10.1038/nrm3151 (2011).
2. Kaksonen, M., Toret, C. P., & Drubin, D. G. A Modular Design for the Clathrin- and Actin-Mediated Endocytosis Machinery. *Cell.* **123** (2), 305–320, doi:10.1016/j.cell.2005.09.024 (2005).
3. Taylor, M. J., Perrais, D., & Merrifield, C. J. A High Precision Survey of the Molecular Dynamics of Mammalian Clathrin-Mediated Endocytosis. *PLoS Biology.* **9** (3), e1000604, doi:10.1371/journal.pbio.1000604.g008 (2011).
4. Ungewickell, E., & Branton, D. Assembly units of clathrin coats. *Nature.* **289** (5796), 420–422 (1981).
5. Bliek, A. M., & Meyerowrtz, E. M. Dynamin-like protein encoded by the Drosophila shibire gene associated with vesicular traffic. *Nature.* **351** (6325), 411–414, doi:10.1038/351411a0 (1991).
6. Hinshaw, J. E., & Schmid, S. L. Dynamin self-assembles into rings suggesting a mechanism for coated vesicle budding. *Nature.* **374** (6518), 190–192, doi:10.1038/374190a0 (1995).
7. Merrifield, C. J., Perrais, D., & Zenisek, D. Coupling between Clathrin-Coated-Pit Invagination, Cortactin Recruitment, and Membrane Scission Observed in Live Cells. *Cell.* **121** (4), 593–606, doi:10.1016/j.cell.2005.03.015 (2005).
8. Grabs, D., Slepnev, V. I., *et al.* The SH3 domain of amphiphysin binds the proline-rich domain of dynamin at a single site that defines a new SH3 binding consensus sequence. *The Journal of biological chemistry.* **272** (20), 13419–13425 (1997).
9. Tosoni, D., Puri, C., *et al.* TTP Specifically Regulates the Internalization of the Transferrin Receptor. *Cell.* **123** (5), 875–888, doi:10.1016/j.cell.2005.10.021 (2005).
10. Puthenveedu, M. A., & Zastrow, von, M. Cargo Regulates Clathrin-Coated Pit Dynamics. *Cell.* **127** (1), 113–124, doi:10.1016/j.cell.2006.08.035 (2006).
11. Soohoo, A. L., & Puthenveedu, M. A. Divergent modes for cargo-mediated control of clathrin-coated pit dynamics. *Molecular Biology of the Cell.* **24** (11), 1725–1734, doi:10.1091/mbc.E12-07-0550 (2013).
12. Posor, Y., Eichhorn-Gruenig, M., *et al.* Spatiotemporal control of endocytosis by phosphatidylinositol-3,4-bisphosphate. *Nature*, doi:10.1038/nature12360 (2013).
13. Mettlen, M., Stoeber, M., Loerke, D., Antonescu, C. N., Danuser, G., & Schmid, S. L. Endocytic accessory proteins are functionally distinguished by their differential effects on the maturation of clathrin-coated pits. *Molecular Biology of the Cell.* **20** (14), 3251–3260, doi:10.1091/mbc.E09-03-0256 (2009).
14. Loerke, D., Mettlen, M., *et al.* Cargo and dynamin regulate clathrin-coated pit maturation. *PLoS Biology.* **7** (3), e1000057 (2009).
15. Axelrod, D. Cell-substrate contacts illuminated by total internal reflection fluorescence. *The Journal of Cell Biology.* **89** (1), 141–145 (1981).
16. Merrifield, C. J., Feldman, M. E., Wan, L., & Almers, W. Imaging actin and dynamin recruitment during invagination of single clathrin-coated pits. *Nature Cell Biology.* **4** (9), 691–698, doi:10.1038/ncb837 (2002).
17. Ehrlich, M., Boll, W., *et al.* Endocytosis by random initiation and stabilization of clathrin-coated pits. *Cell.* **118** (5), 591–605, doi:10.1016/j.cell.2004.08.017 (2004).
18. Yarar, D., Waterman-Storer, C. M., & Schmid, S. L. A dynamic actin cytoskeleton functions at multiple stages of clathrin-mediated endocytosis. *Molecular Biology of the Cell.* **16** (2), 964–975, doi:10.1091/mbc.E04-09-0774 (2005).
19. Rappoport, J. Z., Kemal, S., Benmerah, A., & Simon, S. M. Dynamics of clathrin and adaptor proteins during endocytosis. *American journal of physiology. Cell physiology.* **291** (5), C1072–81, doi:10.1152/ajpcell.00160.2006 (2006).
20. Doyon, J. B., Zeitler, B., *et al.* Rapid and efficient clathrin-mediated endocytosis revealed in genome-edited mammalian cells. *Nature Cell Biology.* **13** (3), 331–337 (2011).
21. Hopp, T. P., Prickett, K. S., *et al.* A Short Polypeptide Marker Sequence Useful for Recombinant Protein Identification and Purification. *Bio/Technology.* **6** (10), 1204–1210, doi:10.1038/nbt1088-1204 (1988).
22. Miesenböck, G., De Angelis, D. A., & Rothman, J. E. Visualizing secretion and synaptic transmission with pH-sensitive green fluorescent proteins. *Nature.* **394** (6689), 192–195, doi:10.1038/28190 (1998).
23. Saffarian, S., Cocucci, E., & Kirchhausen, T. Distinct Dynamics of Endocytic Clathrin-Coated Pits and Coated Plaques. *PLoS Biology.* **7** (9), e1000191, doi:10.1371/journal.pbio.1000191 (2009).
24. Yudowski, G., Puthenveedu, M., Henry, A., & Zastrow, von, M. Cargo-Mediated Regulation of a Rapid Rab4-Dependent Recycling Pathway. *Molecular Biology of the Cell.*, 1–11, doi:10.1091/mbc.E08 (2009).
25. Batchelder, E. M., & Yarar, D. Differential Requirements for Clathrin-dependent Endocytosis at Sites of Cell-Substrate Adhesion. *Molecular Biology of the Cell.* **21** (17), 3070–3079, doi:10.1091/mbc.E09-12-1044 (2010).
26. Mattheyses, A. L., Atkinson, C. E., & Simon, S. M. Imaging Single Endocytic Events Reveals Diversity in Clathrin, Dynamin and Vesicle Dynamics. *Traffic.* **12** (10), 1394–1406, doi:10.1111/j.1600-0854.2011.01235.x (2011).
27. Aguet, F., Antonescu, C. N., Mettlen, M., Schmid, S. L.., & Danuser, G. Advances in analysis of low signal-to-noise images link dynamin and AP2 to the functions of an endocytic checkpoint. *Dev Cell.* **26**(3):279-91. doi: 10.1016/j.devcel.2013.06.019. (2013).
28. Boucrot, E., Howes, M. T., Kirchhausen, T., & Parton, R. G. Redistribution of caveolae during mitosis. *J Cell Sci.* **124**(Pt 12):1965-72. doi: 10.1242/jcs.076570. (2011).
29. Bhaya, D., Davison, M., & Barrangou, R. CRISPR-Cas systems in bacteria and archaea: versatile small RNAs for adaptive defense and regulation. *Annual review of genetics.* **45**, 273–297, doi:10.1146/annurev-genet-110410-132430 (2011).
30. Boch, J., Scholze, H., *et al.* Breaking the Code of DNA Binding Specificity of TAL-Type III Effectors. *Science.* **326** (5959), 1509–1512, doi:10.1126/science.1178811 (2009).

